Non-Adlerian phase slip and nonstationary synchronization of spin-torque oscillators to a microwave source

G. Finocchio,[1,*] M. Carpentieri,[2] A. Giordano,[1] and B. Azzerboni[1]

[1]*Department of Fisica della Materia e Ingegneria Elettronica, University of Messina, C.da di Dio, I-98100, Messina, Italy*

[2]*Department of Elettronica, Informatica e Sistemistica, University of Calabria, Via P. Bucci 42C, I-87036, Rende (CS), Italy*

(Received 5 January 2012; published 30 July 2012)

The nonautonomous dynamics of spin-torque oscillators in the presence of both microwave current and field at the same frequency can exhibit complex nonisochronous effects. A nonstationary mode hopping between quasiperiodic mode (frequency pulling) and periodic mode (phase locking) and a deterministic phase slip characterized by an oscillatory synchronization transient (non-Adlerian phase slip) after the phase jump of $\pm 2\pi$ were predicted. In the latter effect, a wavelet-based analysis reveals that in the positive and negative phase jump the synchronization transient occurs at the frequency of the higher and lower sideband frequency, respectively. The non-Adlerian phase slip effect, even if discovered in STOs, is a general property of nonautonomous behavior valid to any nonisochronous auto-oscillator in regime of moderate and large force locking.

DOI: 10.1103/PhysRevB.86.014438 PACS number(s): 75.75.−c, 85.75.−d

I. INTRODUCTION

In the last decade, a class of nonlinear auto-oscillators, spin-torque-oscillators (STOs),[1] has been extensively studied experimentally[2–5] and theoretically.[6–8] The STO is promising from a technological point of view, being one of the smallest auto-oscillators observed in nature. It also exhibits complex nonlinear dynamics arising from the intrinsic coupling between the oscillator phase and power (the effective magnetic field depends on the spatial distribution of the magnetization).[7]

The main properties of STOs are frequency tunability on bias current and field, narrow linewidth, and high output power. In addition, the nonautonomous dynamical behavior of STOs (in the presence of microwave current or field) can exhibit nonlinear frequency amplitude modulation, frequency pulling, frequency locking, hysteretic and fractional synchronization, and stochastic resonance.[9–14] Analytical, semianalytical, and micromagnetic simulations have been used for the prediction or the explanation of those results, which are mainly in the regime of a "weak" microwave signal, where the oscillator behavior is characterized by isochronous dynamical response, and it is possible to neglect the difference between the instantaneous and the stationary (no microwave signal) oscillation power.[7,15–17] In the nonisochronous regime ("moderate" or "large" microwave signal), analytical theories fail and a complete numerical approach is necessary; synchronization regions are not symmetric and can be overlapped, and strong nonstationary time domain behaviors (transitions to chaos through period doublings of the orbit, unstable intermittent transition from synchronization to chaos, phase slip) are achieved.[18]

We studied the nonisochronous dynamical behavior of STOs in presence of a microwave signal composed by the simultaneous application of microwave current density J_{AC} and field h_{AC}, both at the same frequency.

The key result of this paper is the identification of two dynamical effects in STOs: (i) nonstationary hopping between quasistationary Q (frequency pulling) and periodic P (phase locking) mode[19] (the power spectrum is characterized by two modes with power of the same order, one at the frequency of the microwave source and one near the frequency of the self-oscillation mode); and (ii) phase slip characterized by an oscillatory resynchronization transient after a $\pm 2\pi$ phase jump of the oscillator phase (the power spectrum is characterized by one mode at the frequency of the microwave source and two sidebands). In analogy to the results and the formalism presented in Ref. 20, we called this latter effect non-Adlerian phase slip. A wavelet-based time-frequency study shows that when the phase slip occurs, the sideband modes are nonstationary, being the higher and the lower sideband frequencies related to the oscillator phase jump of $+2\pi$ and -2π, respectively.

The paper is organized as follows: Sec. II introduces the details of the device studied and the numerical implementation of the model, and Secs. III and IV describe the results and the conclusions of our study.

II. NUMERICAL DETAILS

We studied the dynamical behavior of exchange biased spin valves composed of IrMn (8 nm)/Py (10 nm) (polarizer)/Cu (10 nm)/Py (4 nm) (free layer) with an elliptical cross sectional area (120×60 nm) [see inset of Fig. 1(a)]. A Cartesian coordinate system was introduced, where the x and the y axes are related to the easy and the hard in-plane axes of the ellipse, respectively. Our numerical experiment was based on the numerical solution of the Landau–Lifshitz–Gilbert–Slonczweski (LLGS) equation.[1] In addition to the standard effective field (external, exchange, self-magnetostatic), the Oersted field and the magnetostatic coupling with the polarizer were taken into account. The time step used was 32 fs. For a complete description of the numerical techniques see also Ref. 21. Typical parameters for the Py were used: saturation magnetization $M_S = 650 \times 10^3$ A/m, exchange constant $A = 1.3 \times 10^{-11}$ J/m, damping parameter $\alpha = 0.02$, and polarization factor $\eta = 0.3$. The free layer was discretized in computational cells of $5 \times 5 \times 4$ nm^3 (the exchange length is $l_{\mathrm{ex}} = \sqrt{\frac{2A}{\mu_0 M_S^2}} \approx 7$ nm). The bias field was applied out of plane (z direction) with a tilted angle of 10° along the x axis to control the in-plane component of the magnetization [see Fig. 1(a)]. The polarizer was considered fixed along the

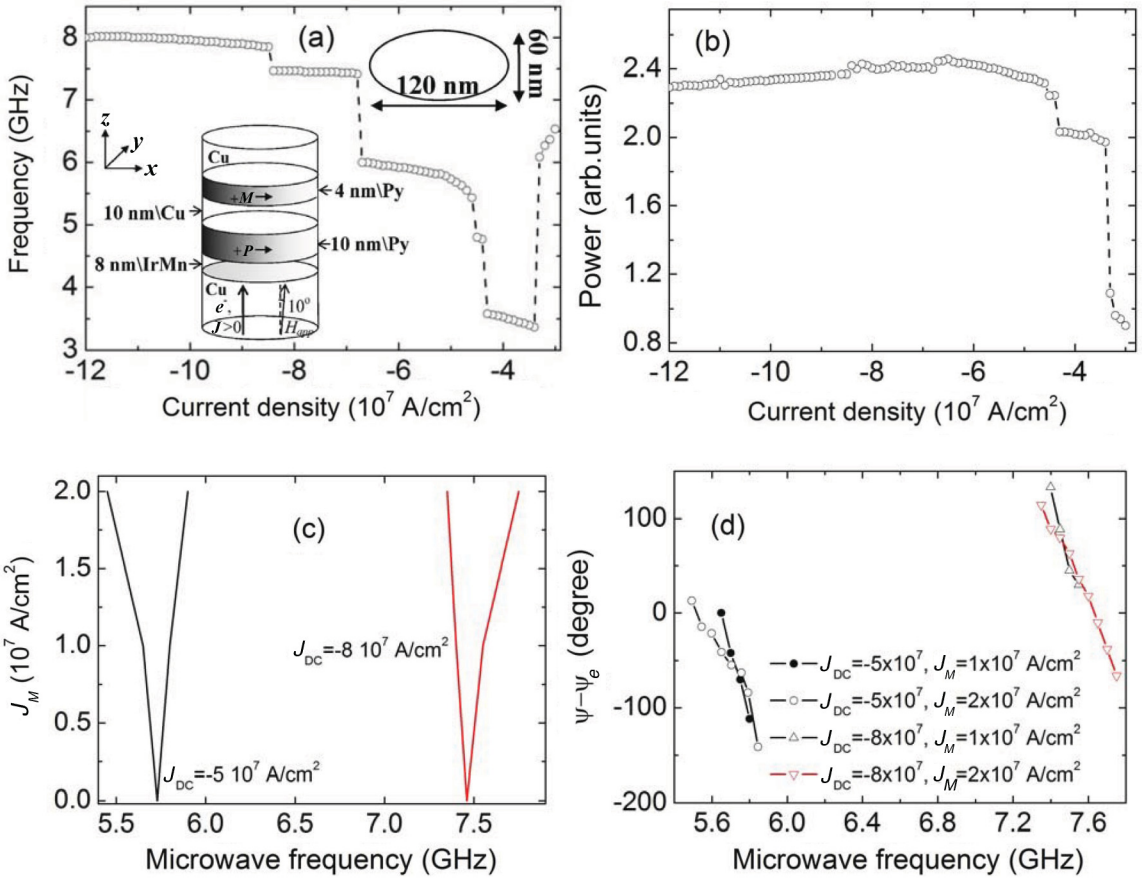

FIG. 1. (Color online) (a) Auto-oscillation frequency f_0 as function of the current density ($H = 200$ mT) (inset: sketch of the studied device); (b) integrated output power as a function of the current density; (c) locking regions computed for $J = -5$ and -8×10^7 A/cm^2 (only a microwave current is applied); (d) intrinsic phase shift Ψ_I between the phase of self-oscillation and the microwave current in the locking region of Fig. 1(c) (both $J = -5$ and -8×10^7 A/cm^2) for $J_M = 1$ and 2×10^7 A/cm^2.

x direction. To study the locking, we considered a microwave current $J_{AC} = J_M \sin(2\pi f_{AC} t + \pi/2)$ ($J_M \leqslant 2 \times 10^7$ A/cm^2) and a microwave field linearly polarized at $\pi/4$ in the xy plane $h_{AC} = h_M \sin(2\pi f_{AC} t + \pi/4)\hat{x} + h_M \sin(2\pi f_{AC} t + \pi/4)\hat{y}$ ($h_M \leqslant 3$ mT). This microwave field can be generated by using the experimental technique developed in Ref. 12. The computational data presented in the rest of the article were obtained with with no thermal effects.

III. RESULTS AND DISCUSSIONS

A. Free running data

First we characterized the STO in the free running regime (no microwave signal). Persistent magnetization oscillation was observed in a wide range of current density and for out-of-plane bias field larger than 180 mT. Here we discuss in detail data for a bias field of 200 mT, but qualitative similar results have been also achieved for 180 and 220 mT. Figures 1(a) and 1(b) display current density J dependence of the oscillation frequency (f_0) and the integrated output power for the giant magnetoresistive (GMR) signal ($H = 200$ mT). The f_0 vs J curve is characterized by red shift and an in-plane oscillation axis up to $J_1 = -3.4 \times 10^7$ A/cm^2, while for $|J| > |J_1|$ the magnetization precesses around an out-of-plane axis (blue shift). The discontinuities observed in the data are related to oscillation axis jumps.[22,24]

B. Isochronous synchronization

We systematically studied the locking region to the first harmonic (the same of the self-oscillation) as function of J_M and h_M in the blue shift region. Figure 1(c) shows the locking region computed for $J = -5$ and -8×10^7 A/cm^2 and related to a microwave current only ($h_M = 0$ mT). The response can be considered in the regime of a "weak" microwave signal; in fact, the locking regions are symmetric and the locking band is linearly dependent on J_M. As already predicted,[23] it is also found an intrinsic phase shift Ψ_I between the phase of the self-oscillation Ψ and the phase of the microwave current Ψ_E in the whole locking region. Figure 1(d) summarizes Ψ_I as function of f_{AC}; as can be observed a linear relationship is achieved and, depending on f_{AC} and J_M, Ψ_I, can also assume the value 0 or $\pi/2$.

C. Nonisochronous synchronization

As will be discussed, when both microwave current and field are applied simultaneously at the same frequency, the nonautonomous response becomes more complicated and

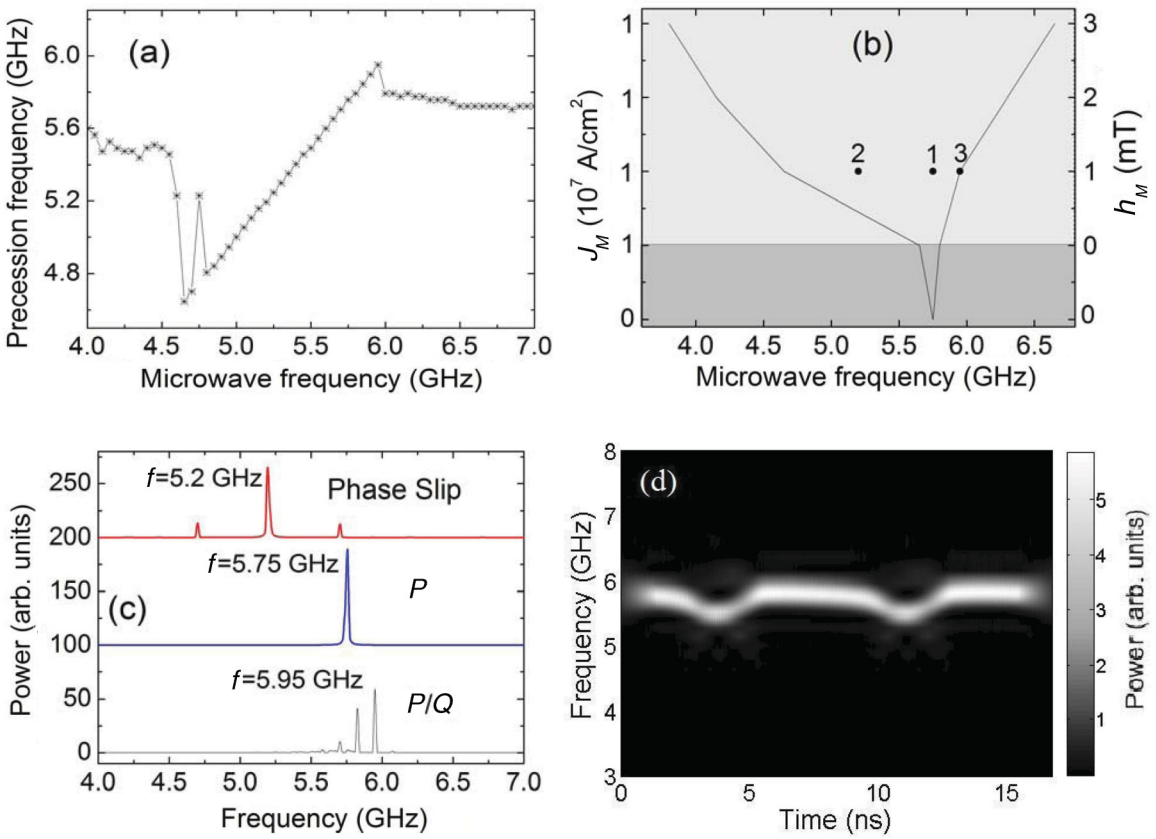

FIG. 2. (Color online) (a) Frequency of the main excited mode (the mode with the largest power) as a function of the microwave frequency computed for $J = -5 \times 10^7$ A/cm^2, $J_M = 1 \times 10^7$ A/cm^2, and $h_M = 1$ mT; (b) locking region computed for $J = -5 \times 10^7$ A/cm^2; (c) power spectra for P mode ($f_{AC} = 5.75$ GHz, point 1), P/Q nonstationary mode ($f_{AC} = 5.95$ GHz, point 3), and non-Alderian phase slip ($f_{AC} = 5.2$ GHz, point 2), $J_M = 1 \times 10^7$ A/cm^2, and $h_M = 1$ mT as indicated in (b); (d) wavelet transform of the time trace of the GMR signal related to the P/Q mode of (c).

nonisochronous effects are observed in the locking region. Figure 2(a) shows the dependence of the frequency of the excited mode with the larger power as a function of the microwave frequency for $J = -5 \times 10^7$ A/cm^2, $J_M = 1 \times 10^7$ A/cm^2, and $h_M = 1$ Mt. The presence of the microwave field gives rise to an increasing of the locking region (from 150 MHz at $h_M = 0$ mT up to 1.3 GHz for $h_M = 1$ mT) and to a behavior different from the one described in Figs. 1(c) and 1(d). We performed a systematic study to better understand the origin of this dynamical behavior, and Fig. 2(b) summarizes the locking region ($J = -5 \times 10^7$ A/cm^2) computed up to $J_M = 1 \times 10^7$ A/cm^2 ($h_M = 0$ mT) and then increasing h_M up to 3 mT, maintaining fixes $J_M = 1 \times 10^7$ A/cm^2. The border lines have been computed considering the last microwave frequency where a mode at the frequency of the microwave source with large power is excited. This locking region is asymmetric, and at some microwave frequencies the power spectrum cannot be identified as a regular P mode [see Fig. 2(c)]. The results obtained for $J = -5 \times 10^7$ A/cm^2 ($J_M = 1 \times 10^7$ A/cm^2 and $h_M = 1$ mT) are discussed in detail. Figure 2(c) shows the power spectra related to points 1–3 depicted in Fig. 2(b). The spectrum for $f_{AC} = 5.75$ GHz (point 1) is a regular P mode, and the spectra at 5.95 GHz (point 3) and 5.2 GHz (point 2) are evidence of the strong nonisochronisms; in fact together with the mode with the large power at the microwave frequency (locking regime), an additional large power mode or two sidebands are excited, respectively. Qualitative similar results have been also obtained up to $J = -9.5 \times 10^7$ A/cm^2 and for $h_M = 2$–3 mT and $J_M = 1.5$ and 2×10^7 A/cm^2.

The origin of this nonisochronism can be understood by means of a time-frequency study of the GMR-signal based on the wavelet transform. We used the complex Morlet as the mother wavelet:

$$\psi_{u,s} = \frac{1}{\sqrt{s\pi f_B}} e^{j2\pi f_c\left(\frac{t-u}{s}\right)} e^{-\left(\frac{t-u}{s}\right)^2/f_B}, \tag{1}$$

where f_C and f_B are two parameters that characterize the mother wavelet function, and s and u are the scale and the shift parameters, respectively. The wavelet transform $W_r(u,s)$ is computed as

$$W_r(u,s) = \frac{1}{\sqrt{s}} \int_{-\infty}^{+\infty} r(t)\psi^*\left(\frac{t-u}{s}\right) dt, \tag{2}$$

where $r(t)$ is the time domain GMR signal, and ψ^* is the complex conjugate of the mother wavelet (see Ref. 24 for all the computational details). Figure 2(d) displays the wavelet scalogram [the modulus of $W_r(u,s)$] for the time trace related to point 3 in Fig. 2(b), with $f_C = 1$ and $f_B = 300$ (the amplitude increases from black to white). The wavelet analysis shows a

mode hopping between the two modes; that is in some time ranges (for example, 5.5–9 ns) the P mode (phase locking) is excited while in other time ranges (for example, 9.5–11.5 ns) the Q mode (frequency pulling) is excited (the main mode has the frequency near the self-oscillation mode and a low power peak at the microwave frequency). We refer to this behavior as nonstationary P/Q mode. The relative power of the two modes depends on how long they are excited, for example, at $f_{AC} = 5.95$ GHz the power of the P mode is larger than that of the Q mode.

In several nonlinear systems a diffuse nonisochronous effect called phase slip is observed.[25,26] It is characterized by brief periods of resynchronization after a phase jump of $\pm 2\pi$ of the oscillator phase. Commonly, after the phase jump the resynchronization transient occurs asymptotically (Adlerian phase slip).[23] In contrast, here we observe in the locking region the P mode coupled with two sidebands. The wavelet transform of those time domain GMR signals displayed in Fig. 3(a) for $f_{AC} = 5.2$ GHz [point 2 of Fig. 2(b)] indicates the nonstationary excitation of the sideband modes, the result of which is completely different from the modulation processes where the sideband modes are stationary.[9,15] In particular, the time evolution of the oscillation phase Ψ is characterized by the occurrence of a phase slip with an oscillatory synchronization transient we called non-Adlerian phase slip [Fig. 3(b) summarizes those computations for 2 ns]. The origin of the nonstationary sidebands is related to the fact that the higher and lower sideband modes are connected to the resynchronization frequency of a $+2\pi$ or -2π phase slip.

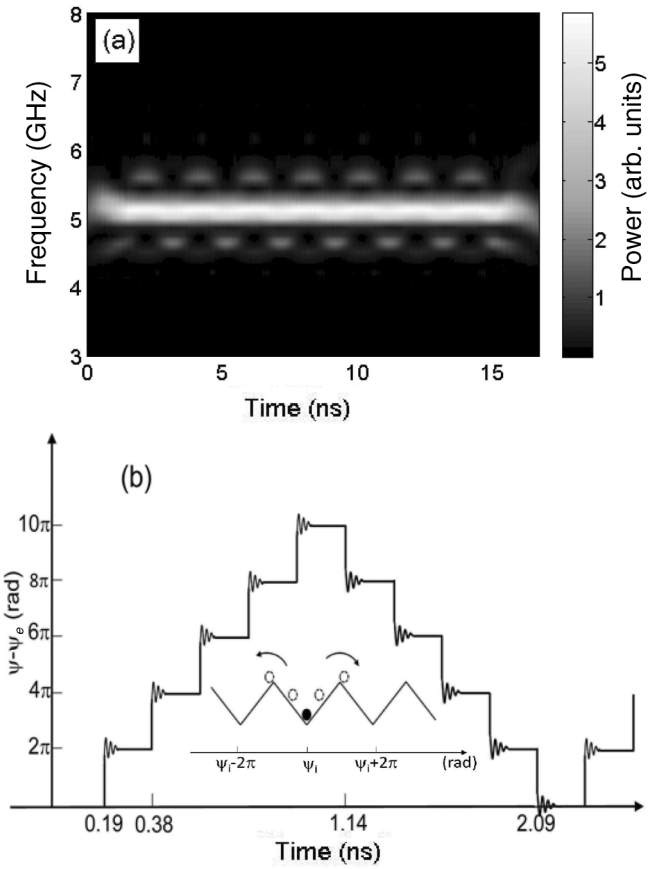

FIG. 3. (a) Wavelet scalogram (white/black color corresponds to the largest/smallest wavelet coefficient amplitude) for $J = -5 \times 10^7$ A/cm^2 and $J_M = 1 \times 10^7$ A/cm^2 and $h_M = 1$ mT at the frequency of $f = 5.2$ GHz. (b) Time domain evolution of the phase of the oscillator. Inset: example of energy landscape where it is possible to observe positive or negative phase jump.

From a theoretical point of view, the linewidth of a regular P mode coincides with the one of the microwave source. The phase slip introduces an additional intrinsic dissipation mechanism that can be seen as an enhancement of the oscillator linewidth and should be taken into account in the design of arrays of STOs, which should work synchronized. The presence of the phase slip can also explain, for example, the experimental evidence of the linewidth enhancement in the power spectrum of STOs near the boundary of the locking region [see Fig. 3(d) of Ref. 13] and the thermally induced sideband observed in Ref. 27.

The phase slip achieved here is periodic (deterministic phase slip) at the same frequency of the microwave source and different from the one obtained in a nonlinear system where the thermal fluctuations are responsible for the phase jumps among different energetic minima (stochastic phase slip). To understand the origin of the observed deterministic phase slip, we introduce the simple scenario displayed in the inset of Fig. 3(b); when the oscillation induced by the microwave source is large enough to overcome the energy barrier that separates two different minima (this is achieved for some value of f_{AC}), the phase slip occurs.

In addition, our computations suggest that the discontinuities in the free running data reduce the amplitude of the microwave source to apply in order to excite the phase slip and the nonstationary P/Q mode. In fact, the synchronization data (by using the same microwave signals) achieved for an out-of-plane bias field larger than 400 mT, where discontinuities in the free running data disappear, are similar to the results already published and described analytically in the regime of a "weak" microwave signal (see, for example, Ref. 7 for a review).

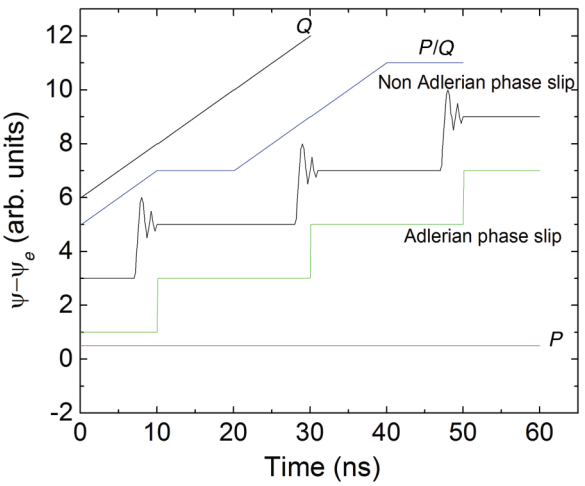

FIG. 4. (Color online) Time evolution of the oscillator phase for different excited modes: Q mode, nonstationary P/Q mode, non-Adlerian and Adlerian phase slip, and P mode.

IV. SUMMARY AND CONCLUSIONS

Figure 4 summarizes qualitatively the time dependence of the oscillator phase for the Q mode (frequency pulling), where Ψ_I increases linearly; the P mode (phase locking), where Ψ_I is constant; the nonstationary P/Q region, where a time domain mode hopping exists between Q and P modes (the phase can be constant or increase linearly); and the Adlerian and non-Adlerian phase slip (abrupt jumps of 2π in the oscillator phase are observed together to asymptotic and oscillatory resynchronization).

In summary, in the nonautonomous behavior of STOs by means of micromagnetic simulations and time-frequency domain analysis based on wavelet transform, the presence of the nonstationary P/Q modes and non-Adlerian phase slip was found. The key finding was the possibility of driving deterministic phase slip by means of the application of a moderate microwave source that could be easily generated experimentally. We think our results can stimulate future experimental studies of the nonisochronisms in self-oscillators such as nonstationary behavior and phase slip not thermally activated. Finally, we identified a phase slip with an oscillatory resynchronization transient, non-Adlerian phase slip, that even if discovered in STOs, is a general property of nonautonomous behavior valid for any auto-oscillator in regime of moderate and large amplitude microwave signal.

ACKNOWLEDGMENTS

This work was supported by Spanish Project under Contract No. MAT2011-28532-C03-01. The authors would like to thank Sergio Greco for his support with this research.

*Corresponding author: gfinocchio@unime.it

[1] J. C. Slonczewski, J. Magn. Magn. Mater. **159**, L1 (1996).
[2] S. I. Kiselev, J. C. Sankey, I. N. Krivorotov, N. C. Emley, R. J. Schoelkopf, R. A. Buhrman, and D. C. Ralph, Nature **425**, 380 (2003).
[3] W. H. Rippard, M. R. Pufall, S. Kaka, S. E. Russek, and T. J. Silva, Phys. Rev. Lett. **92**, 027201 (2004).
[4] A. M. Deac, A. Fukushima, H. Kubota, H. Maehara, Y. Suzuki, S. Yuasa, Y. Nagamine, K. Tsunekawa, D. D. Djayaprawira, and N. Watanabe, Nature Phys. **4**, 803 (2008).
[5] D. Houssameddine, U. Ebels, B. Delaët, B. Rodmacq, I. Firastrau, F. Ponthenier, M. Brunet, C. Thirion, J.-P. Michel, L. Prejbeanu-Buda, M.-C. Cyrille, O. Redon, and B. Dieny, Nat. Mater. **6**, 441 (2007).
[6] G. Bertotti, C. Serpico, I. D. Mayergoyz, A. Magni, M. d'Aquino, and R. Bonin, Phys. Rev. Lett. **94**, 127206 (2005).
[7] A. Slavin and V. Tiberkevich, IEEE Trans. Magn. **45**, 1875 (2009).
[8] G. Finocchio, G. Siracusano, V. Tiberkevich, I. N. Krivorotov, L. Torres, and B. Azzerboni, Phys. Rev. B **81**, 184411 (2010).
[9] M. R. Pufall, W. H. Rippard, S. Kaka, T. J. Silva, and S. E. Russek, Appl. Phys. Lett. **86**, 082506 (2005).
[10] W. H. Rippard, M. R. Pufall, S. Kaka, T. J. Silva, and S. E. Russek, Phys. Rev. Lett. **92**, 027201 (2004).
[11] B. Georges, J. Grollier, M. Darques, V. Cros, C. Deranlot, B. Marcilhac, G. Faini, and A. Fert, Phys. Rev. Lett. **101**, 017201 (2008).
[12] P. Tabor, V. Tiberkevich, A. Slavin, and S. Urazhdin, Phys. Rev. B **82**, 020407(R) (2010).
[13] S. Urazhdin, P. Tabor, V. Tiberkevich, and A. Slavin, Phys. Rev. Lett. **105**, 104101 (2010).
[14] G. Finocchio, I. N. Krivorotov, X. Cheng, L. Torres, and B. Azzerboni, Phys. Rev. B **83**, 134402 (2011).
[15] G. Consolo, V. Puliafito, G. Finocchio, L. Lopez-Diaz, R. Zivieri, L. Giovannini, F. Nizzoli, G. Valenti, and B. Azzerboni, IEEE Trans. Magn. **46**, 3629 (2010).
[16] R. Bonin, G. Bertotti, C. Serpico, I. D. Mayergoyz, and M. d'Aquino, Eur. Phys. J. B **68**, 221 (2009).
[17] M. Carpentieri, G. Finocchio, B. Azzerboni, and L. Torres, Phys. Rev. B **82**, 094434 (2010).
[18] See P. Maffezzoni, IEEE Trans. Comput.-Aided-Design Integrated Circuits Syst. **29**, 1849 (2010), and references therein.
[19] In the regime of isochronisms, an STO with f_0 as a stationary oscillation frequency can exhibit different behavior depending on the frequency f_{AC} of the microwave signal such as frequency pulling and phase locking. The frequency pulling occurs when the f_{AC} approaches f_0 and a quasistationary mode or Q mode is excited (the power spectrum is characterized by two modes, one near f_0 and one with lower power at f_{AC}). The phase locking occurs when the oscillation frequency f_0 is locked at the frequency of the external microwave source f_{AC} and a periodic mode or P mode is excited (the power spectrum is characterized by a single mode at f_{AC}).
[20] Y. Zhou, V. Tiberkevich, G. Consolo, E. Iacocca, B. Azzerboni, A. Slavin, and J. Åkerman, Phys. Rev. B **82**, 012408 (2010).
[21] A. Romeo, G. Finocchio, M. Carpentieri, L. Torres, G. Consolo, and B. Azzerboni, Physica B **403**, 464 (2008); E. Martinez, L. Torres, L. Lopez-Diaz, M. Carpentieri, and G. Finocchio, J. Appl. Phys. **97**, 10E302 (2005); A. Giordano, G. Finocchio, L. Torres, M. Carpentieri, and B. Azzerboni, *ibid.* **111**, 07D112 (2012). See also http://www.ctcms.nist.gov/~rdm/mumag.org.html standard problem #4 report by E. Martinez, L. Torres, and L. Lopez-Diaz.
[22] I. N. Krivorotov, D. V. Berkov, N. L. Gorn, N. C. Emley, J. C. Sankey, D. C. Ralph, and R. A. Buhrman, Phys. Rev. B **76**, 024418 (2007).
[23] Y. Zhou, J. Persson, S. Bonetti, and J. Åkerman, Appl. Phys. Lett. **92**, 092505 (2008).
[24] G. Siracusano, G. Finocchio, A. La Corte, G. Consolo, L. Torres, and B. Azzerboni, Phys. Rev. B **79**, 104438 (2009).
[25] A. Pikovsky, M. Rosenbblum, and J. Kurths, *Synchronization: A Universal Concept in Nonlinear Sciences* (Cambridge, New York, 2001).
[26] Z. Zheng, G. Hu, and B. Hu, Phys. Rev. Lett. **81**, 5318 (1998).
[27] M. d'Aquino, C. Serpico, R. Bonin, G. Bertotti, and I. D. Mayergoyz, Phys. Rev. B **82**, 064415 (2010).